JOURNAL OF SOLID STATE CHEMISTRY 54, 365–377 (1984)

Tungsten Bronze Formation by the Group IIIA Metals*

T. EKSTRÖM

Department of Inorganic Chemistry, Arrhenius Laboratory, University of Stockholm, S-10691 Stockholm, Sweden

M. PARMENTIER

Laboratoire de Chimie du Solide Minéral, Université de Nancy I, Boite Postale 239, 54506 Vandoeuvre les Nancy Cedex, France

K. A. WATTS

School of Materials Science, University of Bradford, Bradford BD7 1DP. West Yorkshire, Great Britain

AND R. J. D. TILLEY

Department of Metallurgy and Materials Science, University College, Newport Road, Cardiff CF2 1TA, Great Britain

Received March 14, 1984

Attempts have been made to prepare tungsten bronze phases from the Group IIIA metals, Al, Ga, and In. Of these, only In seems to from bronzes with any facility and three distinct compounds were characterized. Two of these were perovskite-type phases, one of tetragonal symmetry, with lattice parameters $a = 0.3714$ nm, $c = 0.3870$ nm, which forms below 1173 K and one of orthorhombic (pseudotetragonal) symmetry, with lattice parameters $a = 0.3696$ nm, $b = 0.3722$ nm, and $c = 0.3859$ nm, which forms above 1173 K. Both of these have a composition of approximately $In_{0.02}WO_3$. The third phase which formed in this system was a hexagonal tungsten bronze which has been characterized already. In neither the Al–W–O or the Ga–W–O systems were stable bronzes formed, but some evidence suggested that metastable perovskite bronzes may form in the Ga–W–O system in some circumstances. The formation of these phases is discussed and related to the formation of tungsten bronzes in general.

Introduction

The relationship between structure and stoichiometry in the ternary tungsten oxides is of interest to the crystal chemist in view of the large number of nonstoichiometric phases which form and the differing strategies that these compounds adopt in accommodating the changes in anion to cation ratio (*1*). One group of compounds of particular interest are the tungsten bronzes, of formula M_xWO_3, as their electrical conductivity together with their inertness to oxidizing conditions makes them poten-

* Dedicated to Dr. M. J. Sienko.

0022-4596/84 $3.00

tially useful in display devices, as electrodes and as catalysts. Although a large amount of work has been carried out on the tungsten bronzes, much of which was initiated by M. J. Sienko some 30 years ago, there are still a number of bronze systems which merit further study. Among these are the bronzes of the Group III metals, Al, Ga, In, and Tl.

In the system Al–WO_3, five bronze phases were reported by Pouchard *et al.* (*2*) and the variation of the structure as a function of temperature has been determined (*3*). These bronzes were described as existing over the composition interval Al_xWO_3 up to a value of $x = 0.135$ and they were supposed to have structures in which the Al was interpolated into the cages in the WO_3 host lattice to form "perovskite" bronzes.

There are no literature reports of a bronze in the system Ga–WO_3. In the system In–WO_3 the major phase to form seems to be a hexagonal tungsten bronze phase (*4, 5*). This has a composition in the approximate region of $In_{0.12}WO_3$ to $In_{0.3}WO_3$ and a structure which has been studied in detail (*6, 7*). Only Bouchard and Gillson (*4*) examined the composition region low in In content, and they reported the presence of a tetragonal phase which existed over the composition region $In_{0.01}WO_3$ to $In_{0.05}WO_3$.

In the Tl–WO_3 system Bierstedt *et al.* (*8*) prepared a hexagonal tungsten bronze phase which was further studied by Labbé *et al.* (*6*). The composition region low in the Tl seems to have only been studied by Hussain and Kihlborg, who report a series of intergrowth tungsten bronzes in which lamellae of the hexagonal tungsten bronze structure intergrow with the WO_3 matrix (*9*).

Because of this wide range of behavior, this group of compounds forms a suitable series to investigate the role of atomic parameters on the bronze structure formed, especially at low degrees of metal insertion. However, in order to obtain an accurate knowledge of the microstructures produced, some study by transmission electron microscopy seems to be necessary. This has only been completed in the case of the Tl_xWO_3 bronzes (*9*) and so we have reinvestigated the Al_xWO_3, Ga_xWO_3, and In_xWO_3, by transmission electron microscopy. The results are reported in this paper and discussed in terms of the atomic parameters likely to be important in bronze formation.

Experimental

All samples were prepared by mixing together appropriate amounts of high-purity chemicals supplied by Johnson and Matthey Ltd., of Specpure Grade, or compounds derived from these starting materials. The mixtures were heated in sealed evacuated silica ampoules for the times and temperatures listed in Tables I, II, and III.

Compositions on the Al_xWO_3 line were prepared by heating together Al_2O_3, WO_3, and WO_2 or Al metal and WO_3 powder. Compositions on the Ga_xWO_3 line were prepared by heating Ga metal and WO_3; Ga_2O_3, WO_3 and WO_2 or Ga_2O, WO_3, and W metal. Further details of the procedure used for these phases are contained in the Results section. Compositions on the In_xWO_3 line were prepared from In metal and WO_3 or In_2O_3, WO_3, and WO_2. In some of these samples a preliminary heating at 673 K for several days was carried out before the temperature was raised to the desired final reaction temperature.

After preparation all samples were examined by optical microscopy using a Zeiss Ultraphot microscope, and by powder X-ray diffraction using a Hägg–Guinier focussing camera employing strictly monochromatic Cu$K\alpha_1$ radiation and KCl ($\lambda = 0.6292$ nm) as an internal standard. The positions of lines on the films were estimated visually or by means of an Abrahamsson automatic film scanner. Evaluation of the film data,

line indexing, and refinement of the unit cell parameters were performed by computer using programs written by Brandt and Nord (*10*).

Many samples were examined by high-resolution electron microscopy using a JEM 100B electron microscope fitted with a goniometer stage and operated at 100 kV or a JEM 200CX electron microscope fitted with a top-entry goniometer stage and operated at 200 kV. For this, selected portions of the samples were crushed under *n*-butanol in an agate mortar. A drop of the resultant suspension was then allowed to dry on a net-like carbon film supported on a copper grid. Crystal fragments which projected over holes in the net were examined.

In addition some samples were examined by scanning electron microscopy using an ISI Super IIIA electron microscope fitted with a PGT EDAX analysis system. Further samples were analyzed with a Philips EM 400T transmission electron microscope fitted with a LINK 290 Energy Dispersive X-ray analysis unit or a JEOL JSM 35C5 scanning electron microscope also fitted with a LINK systems EDAX analysis system.

Results

Al_xWO_3

The compositions prepared and the heating times and temperatures employed in the attempts to form an Al_xWO_3 bronze are listed in Table I. It should be noted that the

TABLE I

SAMPLES PREPARED IN THE Al–W–O SYSTEMS

Gross composition	Preparation		X-Ray phase analysis[a]
	Temp, °K	Time, days	
$Al_{0.01}WO_3$	1173	7	WO_3, (disordered *CS* phases)
		60	WO_3, (disordered *CS* phases)
$Al_{0.02}WO_3$	1173	7[b]	WO_3, (disordered *CS* phases)
$Al_{0.025}WO_3$	1223	7	WO_3, (disordered *CS* phases)
		21	WO_3, (disordered *CS* phases)
	1373	7	WO_3, (disordered *CS* phases) ((?))
		21	WO_3, (disordered *CS* phases) ((?))
$Al_{0.03}WO_3$	1173	7	WO_3, disordered *CS* phases
		60	Disordered *CS* phases, (WO_3)
$Al_{0.05}WO_3$	1173	7	Disordered *CS* phases, ($(Al_2(WO_4)_3)$)
		7[b]	$WO_{2.83}$, (disordered *CS* phases)
		60	Quasiordered *CS* phases, ((WO_3))($(Al_2(WO_4)_3)$)
$Al_{0.07}WO_3$	1173	7	Quasiordered *CS* phases, $Al_2(WO_4)$
		60	Quasiordered *CS* phases, $Al_2(WO_4)$
$Al_{0.1}WO_3$	1173	7[b]	$WO_{2.83}$, ((disordered *CS* phases))
$Al_{0.11}WO_3$	1223	7	
		21	Quasiordered *CS* phases, (?)
	1373	7	$WO_{2.83}$, $W_{18}O_{49}$, (quasiordered *CS* phases)
		21	$WO_{2.83}$, θ(Al)

Note. The θ(Al) represents a phase with the Mo_5O_{14} structure (see Ref. (*13*)), all other phases are described in Ref. (*14*). $WO_{2.83}$ represents a disordered phase similar to $W_{24}O_{68}$ (see Ref. (*14*)).

[a] (A) and ((A)) represent small and very small amounts of phase A deduced from the intensity of the X-ray patterns.

[b] All these samples have undergone a preliminary heating of 3 days at 873 K and were prepared from Al metal and WO_3 powder. All others were prepared from Al_2O_3, WO_3, and WO_2.

starting materials were in some cases Al_2O_3, WO_3, and WO_2 and in other cases Al metal and WO_3. This is because in initial experiments using Al_2O_3 as the source of Al no bronze phases were found. As this result was in disagreement with that reported by Pouchard *et al.* (*2, 3*) who used Al metal we repeated some experiments with Al and WO_3 as starting materials, following the preparation described by these latter authors as far as possible. It was found, however, that under the conditions employed in our experiments an Al_xWO_3 bronze did not form. Microanalysis showed no trace of Al in the reaction products except in a few nodules of a grey Al-rich oxide.

From the X-ray results it would appear that the Al_2O_3 oxide reacted with the WO_3 to form an intermediary compound as reported by Waring (*11*). A subsequent structure determination by Craig and Stephenson (*12*) showed the formula of this oxide to be $Al_2(WO_4)_3$. The remaining materials in the reaction mixture were then reduced tungsten oxides, WO_{3-x}, of appropriate stoichiometry. In keeping with our previous observations (*13*) any WO_3 present in the reacted materials was found as both monoclinic and orthorhombic modifications. However, this seems due to the presence of low densities of {102} *CS* planes rather than interpolated Al in the WO_3 structure. The products formed in our experiments are summarized on the phase diagram shown in Fig. 1a.

Ga_xWO_3

Initial experiments suggested that if a Ga_xWO_3 bronze formed in the Ga–WO_3 system it was, at best, metastable. Because

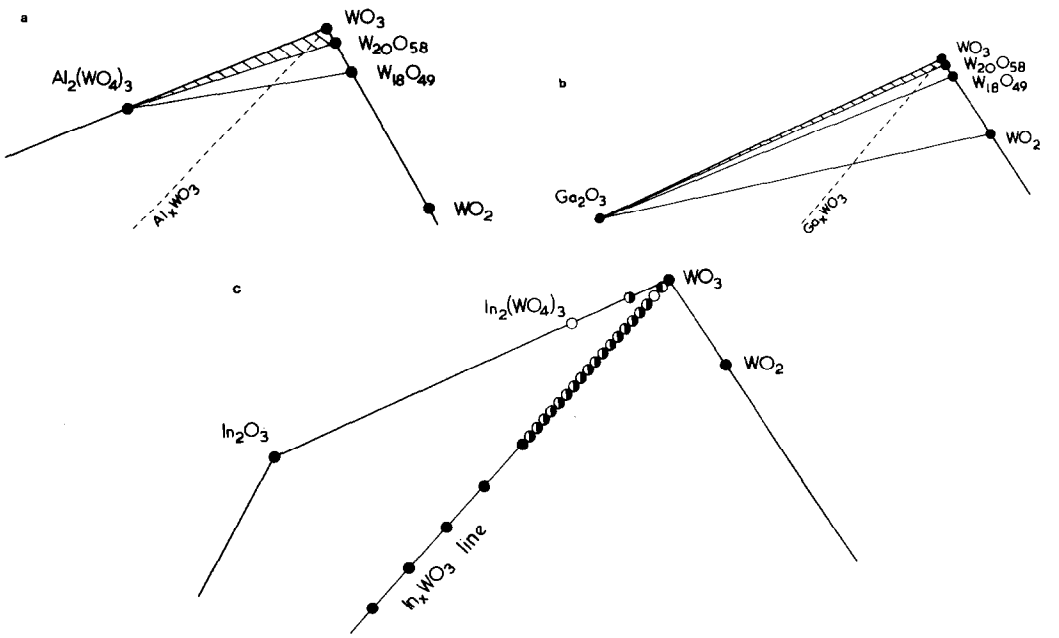

FIG. 1. Existence diagrams showing the phases present in sealed-tube preparations in the systems (a) Al–W–O, (b) Ga–W–O and (c) In–W–O at temperatures close to 1073 K. These diagrams may not represent the equilibrium phase diagrams for these systems. In (c) the circles represent the gross compositions prepared. Open or filled circles represent samples which were apparently monophasic according to powder X-ray diffraction while half-filled circles represent samples containing two or three phases.

of this a large number of preparations were attempted, utilizing low heating temperatures and short heating times as well as a variety of starting materials in order to determine if such metastable bronzes did form. These preparations are listed in Table II. The first group of experiments were aimed at exploring the possible temperature stability of a potential bronze phase. Samples were prepared from Ga metal and WO_3 with an overall composition $Ga_{0.08}WO_3$ and heated at temperatures from 873 to 1673 K. In the temperature range 873 to 1173 K samples were examined after 1 day, reground and reexamined after a further 2 days of heating, and then reground and reheated for another 18 days. In order to check whether a possible bronze phase had a transitory existence, as has been found for Zr_xWO_3 bronzes (*15*) the specimens heated at 923, 1273, and 1673 K were examined after $\frac{1}{2}$ hr, 1 hr, and 1 day. The samples heated at 1273 and 1673 K appeared to be fully reacted and after only 1 hr of heating and apart from a continuing attack on the silica, nothing more happened on further heating.

In order to explore composition variation, samples of compositions between $Ga_{0.01}WO_3$ to $Ga_{0.20}WO_3$ prepared from Ga metal and WO_3 were heated at 1173 K for 1 day, reground and then heated for a further 3 weeks. Some of these were further heated for up to 60 days. Other samples were prepared from Ga_2O_3, WO_3, and WO_2, heated to 873 K for an initial period of 3 days and then to 1173 K for a further 7 days.

Besides these preparations a number of other attempts were made to prepare samples under a variety of conditions which included low pressure of water vapor, approximately 4 bar, at a preparation temperature of 1173 K, and the use of specially prepared Ga_2O. In addition, mixtures of Ga_2O_3 and WO_3 were heated to check on whether a tungstate formed which could be used as an intermediate phase in the preparation of a bronze, but no such compound was isolated.

All of the results obtained in these experiments were the same. The products of reaction were generally reduced tungsten oxides, either crystallographic shear phases, $W_{24}O_{68}$ or $W_{18}O_{49}$, together with Ga_2O_3. The overall reaction scheme would thus appear to be

$$2x\ \mathrm{Ga} + \mathrm{WO_3} \rightarrow x\mathrm{Ga_2O_3} + \mathrm{WO_{3-3x}}$$

However, there was evidence for the formation of a perovskite bronze in a few of the preparations using Ga_2O_3. In a sample of composition $Ga_{0.03}WO_3$ heated at 1173 K for 7 days an orthorhombic phase was found with a unit cell with $a = 0.738$ nm, $b = 0.748$ nm, and $c = 0.773$ nm. In a preparation of composition $Ga_{0.07}WO_3$ heated for the same amount of time, a tetragonal phase had lattice parameters of $a = 0.524$ nm, $c = 0.388$ nm. In neither sample was the supposed bronze phase pure and the films were complicated by the fact that the WO_3 itself was also present as a mixture of the monoclinic and orthorhombic forms, the latter which we believe to be stabilized by a low density of crystallographic shear phases.

The appearance of these bronze phases was transitory, and rather rare, so that in the bulk of preparations only reduced tungsten oxides and Ga_2O_3 was found. It is possible that other preparation conditions might possibly yield monophasic samples, but this is by no means sure. The results of the phase analysis obtained in this study are summarized in Fig. 1b.

In_xWO_3

In these experiments it was found that if sealed tubes were heated immediately up to 1173 K, severe reaction took place between the silica and the contents and no bronzes formed. If the sample tubes were heated for about 3 days at 873 K before the temperature was increased, bronzes were obtained,

TABLE II

SAMPLES PREPARED IN THE Ga–W–O SYSTEM

Gross composition	Preparation		X-Ray phase analysis
	Temp, °K	Time, days	
$Ga_{0.01}WO_3$	1173	7	WO_3, (Ga_xWO_3 *o*-rh)
		21[a]	WO_3, (disordered *CS*)
		60	WO_3, (disordered *CS*)
$Ga_{0.02}WO_3$	1173	7[b]	WO_3, ((?))
		21[a]	WO_3, (disordered *CS*)
$Ga_{0.03}WO_3$	1173	7	Ga_xWO_3 o-rh, (WO_3)
		21[a]	WO_3, disordered *CS*
		60	WO_3, disordered *CS*
$Ga_{0.04}WO_3$	1173	21[a]	Disordered and quasiordered *CS*
$Ga_{0.05}WO_3$	1173	7	Ga_xWO_3 o-rh, disordered *CS*
		21[a]	Disordered and quasiordered *CS*, $WO_{2.83}$, ((Ga_2O_3))
		60	Disordered and quasiordered *CS*, $WO_{2.83}$, ((Ga_2O_3))
$Ga_{0.06}WO_3$	1173	21[a]	Quasiordered *CS*, $W_{18}O_{49}$, ((Ga_2O_3))
$Ga_{0.07}WO_3$	1173	7	Ga_xWO_3 tetr, quasiordered *CS*
		21[a]	Quasiordered *CS*, ($W_{18}O_{49}$), (Ga_2O_3)
		60	Quasiordered *CS*, $WO_{2.83}$, (Ga_2O_3)
$Ga_{0.08}WO_3$	873	1	WO_3, disordered *CS*, $W_{18}O_{49}$
		3	$W_{18}O_{49}$, (Ga_2O_3)
		21	$W_{18}O_{49}$, (Ga_2O_3)
	973	1[c]	WO_3, disordered *CS*, $W_{18}O_{49}$
		3	$W_{18}O_{49}$, (Ga_2O_3)
		8[c]	$W_{18}O_{49}$, (Ga_2O_3)
		21	$W_{18}O_{49}$, (Ga_2O_3)
	1073	1	WO_3, disordered *CS*, $W_{18}O_{49}$
		3	$W_{18}O_{49}$, (Ga_2O_3)
		21[c]	$W_{18}O_{49}$, (Ga_2O_3)
	1173	1[c]	WO_3, disordered *CS*, $W_{18}O_{49}$
		2[d]	$W_{18}O_{49}$, (Ga_2O_3)
		3	$W_{18}O_{49}$, (Ga_2O_3)
		4[d]	$W_{18}O_{49}$, (Ga_2O_3)
		8[d]	$W_{18}O_{49}$, (Ga_2O_3)
		21	$W_{18}O_{49}$, (Ga_2O_3)
	1273	1[e]	$W_{18}O_{49}$, (Ga_2O_3)
	1673	1[c]	$W_{18}O_{49}$, (Ga_2O_3)
$Ga_{0.1}WO_3$	1173	21[a]	$W_{18}O_{49}$, (Ga_2O_3), ((cubic bronze?))
$Ga_{0.12}WO_3$	1173	21[a]	$W_{18}O_{49}$, silica strongly attacked
$Ga_{0.15}WO_3$	1173	21[a]	$W_{18}O_{49}$, silica strongly attacked
$Ga_{0.20}WO_3$	1173	21[a]	$W_{18}O_{49}$, silica strongly attacked

[a] Samples were heated for 1 day and then reground as pretreatment.
[b] Sample heated at 873 K for 3 days as pretreatment.
[c] Also prepared from Ga_2O.
[d] Samples heated under approx. 4 bar H_2O vapor.
[e] Also examined and reground after 1/2 and 1 hr.

although samples did not always appear to have reached true equilibrium, as the X-ray powder patterns sometimes showed more than two phases to be present, when equilibrium would require only one or two phases at most to coexist. The preparations made and the reaction products found are listed in Table III and summarized on Fig. 1c.

The largest number of samples were prepared along the In_xWO_3 line at 1173 K and spanned the composition range from $In_{0.01}WO_3$ to $In_{0.40}WO_3$. These preparations exhibited a large degree of homogeneity and were a dark blue in color. As the In content was increased the samples appeared more crystalline with the crystals showing the metallic luster typical of the tungsten bronzes. This was particularly pronounced for those samples with $x > 0.2$.

TABLE III

SAMPLES PREPARED IN THE In–W–O SYSTEM

Gross composition	Preparation		X-Ray analysis
	Temp, °K	Time, days	
$In_{0.1}WO_3$	1173	3	In_xWO_3 ortho, ((reduced WO_3))
$In_{0.02}WO_3$	1073	7[a]	In_xWO_3 tet
	1173	3	In_xWO_3 ortho, (disordered *CS*)
	1273	7[a]	In_xWO_3 ortho, (disordered *CS*)
$In_{0.03}WO_3$	1173	3	In_xWO_3 ortho, (disordered *CS*), ((HTB))
$In_{0.04}WO_3$	1073	7[a]	In_xWO_3 tet, ((HTB))
	1173	3	disordered *CS*, (HTB), ((In_xWO_3 ortho))
	1273	7[a]	In_xWO_3 ortho, (HTB)
$In_{0.05}WO_3$	1173	3	disordered *CS*, (HTB), ((In_xWO_3 ortho))
$In_{0.06}WO_3$	1073	7[a]	In_xWO_3 ortho, (HTB)
	1173	3	disordered *CS*, (HTB)
	1273	7[a]	In_xWO_3 ortho, (HTB)
$In_{0.07}WO_3$	1173	3	disordered *CS*, (HTB), ((In_xWO_3 ortho))
$In_{0.08}WO_3$	1073	7[a]	In_xWO_3, (HTB)
	1173	3	disordered *CS*, (HTB)
	1273	7[a]	In_xWO_3 ortho, HTB
$In_{0.09}WO_3$	1173	3	In_xWO_3 ortho, HTB
$In_{0.1}WO_3$	1073	7[a]	In_xWO_3 tet, HTB, disordered *CS*,
	1173	7[a]	In_xWO_3 ortho, HTB
	1273	7[a]	HTB, In_xWO_3 ortho
$In_{0.11}WO_3$	1173	7[a]	HTB, In_xWO_3 ortho
$In_{0.12}WO_3$	1173	7[a]	HTB, In_xWO_3 ortho
$In_{0.13}WO_3$	1173	7[a]	HTB, In_xWO_3 ortho
$In_{0.14}WO_3$	1173	7[a]	HTB, In_xWO_3 ortho, In_xWO_3 tet
$In_{0.15}WO_3$	1173	7[a]	HTB, ((In_xWO_3 tet))
$In_{0.16}WO_3$	1173	7[a]	HTB, ((In_xWO_3 tet))
$In_{0.17}WO_3$	1173	7[a]	HTB, (In_xWO_3 tet)
$In_{0.18}WO_3$	1173	7[a]	HTB, (In_xWO_3 tet)
$In_{0.19}WO_3$	1173	7[a]	HTB, ((In_xWO_3 tet))
$In_{0.2}WO_3$	1173	3	HTB
$In_{0.25}WO_3$	1173	7[a]	HTB
$In_{0.35}WO_3$	1173	7[a]	HTB
$In_{0.4}WO_3$	1173	7[a]	HTB

[a] Denotes a preliminary heating of 4 days at 873 K.

In the composition range between $In_{0.01}WO_3$ and $In_{0.03}WO_3$ a perovskite bronze phase formed. However, the situation as revealed by the X-ray films was not straightforward. In compositions In_xWO_3 with $x > 0.03$ the perovskite bronze phase was sometimes of orthorhombic symmetry and sometimes of tetragonal symmetry. However, no trend was observed as a function of composition. Moreover, in neither the tetragonal phase nor the orthorhombic phase were any smooth changes in lattice parameter observed as a function of sample composition. These results suggested that the perovskite bronze phase had only a very narrow compositional extension along the In_xWO_3 line, and that the two forms may be due to temperature dependence rather than composition dependence. This also implied that the transition temperature between the two forms was close to 1173 K.

The phase which coexisted with the perovskite bronze in compositions richer in In than $x > 0.03$ was of the hexagonal tungsten bronze (HTB) type. The amount of this phase present in the preparations increased with In content, up to a composition of about $In_{0.2}WO_3$, after which it existed as the sole phase present. The lower limit of this phase lies therefore in the range between $In_{0.2}WO_3$ and $In_{0.25}WO_3$ at this temperature. The upper phase limit was found to be approximately $In_{0.35}WO_3$. Both of these values are in good agreement with previous studies (*4–7*). As no powder pattern of this phase has been published before an example of a pattern from an HTB phase found in a sample of overall composition $In_{0.4}WO_3$ is given in Table IV. The unit cell size of this material was found to be $a = 0.7363$ nm, $c = 0.7500$ nm.

Electron microscope examination of the HTB phases in a direction parallel to the c axis showed that domain formation was rare and the crystal fragments usually appeared to be well ordered. No traces of diffuse scattering or other signs of short- or long-range order were to be found on the electron diffraction patterns. Examination at higher magnification and resolution did, however, show that the contrast in the hexagonal tunnels was variable. An example of this is shown in Fig. 2. This was believed to be due to variable In populations in tunnels.

TABLE IV

THE X-RAY POWDER DIFFRACTION PATTERNS OF A HEXAGONAL TUNGSTEN BRONZE (HTB) TAKEN FROM A SAMPLE OF OVERALL COMPOSITION $In_{0.40}WO_3$

hkl	d_{obs}	$\sin^2\theta_{obs}$	$\sin^2\theta_{calc}$	$\theta \times 10^{-4}$	I_{obs}
100	0.6370	0.014610	0.014575	0.35	5
101	0.4852	0.025210	0.25116	0.94	1
002	0.3749	0.042220	0.42164	0.56	38
110	0.3683	0.043740	0.43726	0.14	6
111	0.3301	0.054430	0.054267	1.63	2
102	0.3230	0.056840	0.056739	1.01	40
200	0.3186	0.058460	0.058301	1.59	100
201	0.2932	0.068990	0.068842	1.48	1
112	0.2625	0.086060	0.085890	1.70	24
202	0.2428	0.100610	0.100465	1.45	33
211	0.2293	0.112720	0.112567	1.53	35
300	0.2125	0.131280	0.131177	1.03	3
113	0.2067	0.138790	0.138594	1.94	1
212	0.2029	0.144090	0.144190	−1.00	12
203	0.1968	0.153120	0.153170	−0.50	1
004	0.1875	0.168660	0.168656	0.04	17
302	0.1849	0.173510	0.173341	1.69	1
220	0.1842	0.174810	0.174902	−0.92	22
104	0.1799	0.183280	0.183231	0.49	2
310	0.1769	0.189480	0.189477	0.03	4
213	0.1735	0.197050	0.196895	1.55	1
311	0.1722	0.200060	0.200018	0.42	4
114	0.1671	0.212430	0.212381	0.49	2
222	0.1653	0.217040	0.217066	−0.26	16
204	0.1616	0.226990	0.226957	0.33	24
312	0.1601	0.231420	0.231641	−2.21	5
400	0.1595	0.233140	0.233203	−0.63	14
401	0.1561	0.243380	0.243744	−3.64	1
402	0.1468	0.275170	0.275367	−1.97	11
321	0.1434	0.288160	0.287469	6.91	2
304	0.1407	0.299730	0.299832	−1.02	1
410	0.1392	0.306010	0.306079	−0.69	1
411	0.1369	0.316360	0.316620	−2.60	1
322	0.1364	0.318840	0.319092	−2.52	2
224	0.1314	0.343410	0.343558	−1.48	10

Note. Refinement yielded the hexagonal unit cell parameters $a = 0.7363 \pm 2$ nm, $c = 0.7500 \pm 2$ nm.

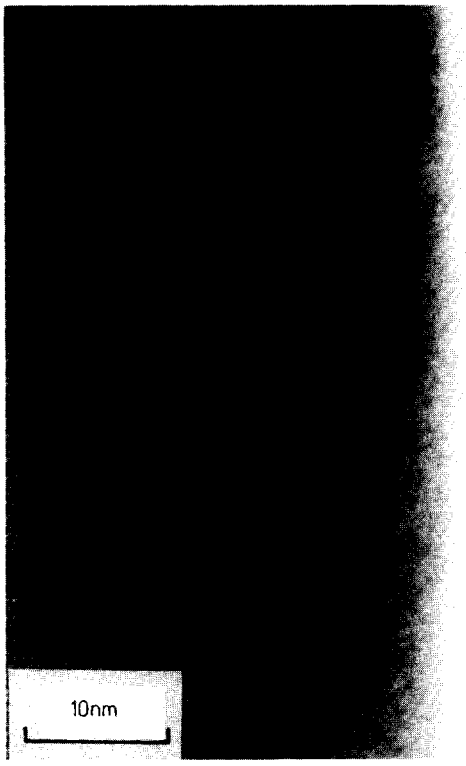

FIG. 2. High-resolution electron micrograph of a fragment of an In_xWO_3 hexagonal tungsten bronze viewed parallel to the hexagonal tunnels, i.e., the c axis. The variable contrast suggests a variable filling of the tunnels by In atoms.

Computer simulation of electron micrographs were in agreement with this interpretation. The HTB specimens were not examined in the direction perpendicular to the c axis in this study although partial ordering along the tunnels has been observed in the past (*16*).

The composition region below the HTB range was also very carefully examined by electron microscopy in the search for intergrowth tungsten bronzes. Despite the fact that many different samples were studied, no evidence was found to suggest that this mode of accommodating nonstoichiometry was utilized here. In order to pursue the symmetry variation of the perovskite bronze phase further, two series of samples were prepared, one at 1073 and one at 1273 K. Samples heated to a final temperature of 1073 K in the composition range $In_{0.02}WO_3$ to $In_{0.1}WO_3$ showed that at the lowest composition the tetragonal phase formed. This seemed to be the only product in $In_{0.02}WO_3$ preparations, and its X-ray powder pattern is recorded in Table V. The unit cell parameters for this phase were found to be a = 0.7398 nm, c = 0.7693 nm. These values are in fair agreement with those of Bouchard and Gillson (*4*) who found a = 0.5233 nm and c = 0.3863 nm for a similar tetragonal phase. Here we note that Bouchard and Gillson took a smaller unit cell, using $a' = a\sqrt{2}$ and $c' = \frac{1}{2}c$. However, we prefer to retain the larger cell to show its relationship to WO_3 and the orthorhombic phases. We found the phase range of this bronze to be slightly less than that reported by these latter authors, as in samples of overall composition In_xWO_3 with $x > 0.02$ the HTB phase was found to be present in increasing amounts as the In content increased. Examination by scanning electron microscopy showed that plate-like crystals occurred in these samples with an In content of 20 to 30%. It seems reasonable to conclude that these are crystals of the HTB phase.

A series of preparations heated to 1273 K over the composition range $In_{0.02}WO_3$ to $In_{0.10}WO_3$ gave similar results. In the $In_{0.02}WO_3$ preparations a perovskite bronze phase was the major product. At these temperatures it showed orthorhombic symmetry rather than tetragonal, but the degree of distortion of the cell away from tetragonal is small, as can be seen from the powder pattern which is shown in Table VI. The unit cell parameters for the phase were found to be a = 0.7367 nm, b = 0.7441 nm, c = 0.7702 nm.

In order to confirm the identity of the orthorhombic and tetragonal phases a sample of $In_{0.02}WO_3$ prepared at 1273 K was reheated at 1073 K and a sample prepared at 1073 K was reheated at 1273 K. The te-

TABLE V

THE X-RAY POWDER DIFFRACTION PATTERN FOR A MONOPHASIC TETRAGONAL PEROVSKITE BRONZE FROM A SAMPLE OF OVERALL COMPOSITION $In_{0.02}WO_3$ HEATED AT 800°C

hkl	d_{obs}	$\sin^2\theta_{obs}$	$\sin^2\theta_{calc}$	$\delta \times 10^{-4}$	I_{obs}
002	0.3846	0.040090	0.040091	−0.01	75
200	0.3697	0.043400	0.043269	1.31	100
210	0.3313	0.054070	0.054086	−0.16	4
112	0.3099	0.061790	0.061725	0.65	32
202	0.2666	0.083500	0.083359	1.41	71
220	0.2616	0.086720	0.086538	1.82	51
212	0.2509	0.094200	0.094177	0.23	4
103	0.2421	0.101170	0.101021	1.49	1
222	0.2163	0.126790	0.126628	1.62	34
213	0.2030	0.143890	0.144290	−4.00	16
312	0.1998	0.148660	0.148263	3.97	11
004	0.1923	0.160310	0.160362	−0.52	10
104	0.1854	0.172400	0.171189	12.11	3
400	0.1844	0.174510	0.173076	14.34	9
114	0.1805	0.181920	0.181997	−0.77	28
204	0.1706	0.203630	0.203631	−0.01	17
402	0.1671	0.212380	0.213166	−7.86	1
214	0.1663	0.214430	0.214448	−0.18	12
420	0.1651	0.217440	0.216344	10.96	13
412	0.1630	0.223310	0.223983	−6.73	3
332	0.1588	0.235040	0.234800	2.40	3
224	0.1549	0.246890	0.246900	−0.10	10
422	0.1520	0.256910	0.256435	4.75	3
304	0.1518	0.257270	0.257717	−4.47	20
314	0.1485	0.268650	0.268534	1.16	18
324	0.1403	0.300990	0.300986	0.04	2
502	0.1382	0.310540	0.310521	0.19	3
512	0.1361	0.320290	0.321338	−10.48	1
521	0.1354	0.323240	0.323722	−4.82	2
404	0.1331	0.334540	0.333438	11.02	4
440	0.1308	0.346540	0.346151	3.89	5
334	0.1292	0.355120	0.355072	0.48	5
424	0.1254	0.377190	0.376707	4.83	5
116	0.1246	0.382170	0.382449	−2.79	6
442	0.1238	0.386640	0.386242	3.98	4

Note. Refinement yielded the lattice parameters for the tetragonal unit cell of $a = 0.7398 \pm 2$ nm, $c = 0.7693 \pm 2$ nm.

tragonal low-temperature phase rapidly transformed to the orthorhombic high-temperature form on heating at 1273 K. The high-temperature form had only partially changed to tetragonal on heating at 1073 K for 12 hr, but the transformation was clearly taking place.

Discussion

The Al–, Ga–, and In–W–O Systems

In the Al–W–O system, no positive evidence was found for bronze formation at all, despite using a variety of starting materials and a range of temperatures and other reaction conditions. Instead, reaction of Al metal appears to lead to the formation of Al_2O_3 and reduced tungsten oxides. Further

TABLE VI

THE X-RAY POWDER DIFFRACTION PATTERN OF A TUNGSTEN BRONZE OF ORTHORHOMBIC SYMMETRY, FROM A SAMPLE OF OVERALL COMPOSITION $In_{0.02}WO_3$

hkl	d_{obs}	$\sin^2\theta_{obs}$	$\sin^2\theta_{calc}$	$\delta \times 10^{-4}$	I_{obs}
002	0.3854	0.039930	0.39959	−0.29	100
020	0.3725	0.042730	0.42800	−0.70	55
200	0.3687	0.043630	0.43666	−0.36	76
201	0.3328	0.053530	0.053656	−1.26	2
112	0.3104	0.061560	0.061576	−0.16	28
022	0.2673	0.083010	0.082759	2.51	31
220	0.2619	0.086420	0.086466	−0.46	39
122	0.2516	0.093680	0.093676	0.04	2
222	0.2166	0.126420	0.126425	−0.05	23
123	0.2030	0.143910	0.143625	2.85	13
132	0.2007	0.147180	0.147175	0.05	5
312	0.1996	0.148950	0.148908	0.42	7
004	0.1926	0.159810	0.159838	−0.28	15
040	0.1861	0.171160	0.171199	−0.39	5
400	0.1843	0.174630	0.174664	−0.34	11
114	0.1808	0.181520	0.181454	0.66	19
204	0.1708	0.203300	0.203504	−2.04	10
042	0.1676	0.211160	0.211158	0.02	6
402	0.1662	0.214730	0.214623	1.07	15
420	0.1651	0.217490	0.217464	0.26	13
332	0.1590	0.234540	0.234507	0.33	3
224	0.1551	0.246340	0.246303	0.37	7
242	0.1525	0.254800	0.254824	−0.24	6
422	0.1518	0.257430	0.257423	0.07	11
314	0.1485	0.268870	0.268786	0.84	11

Note. Refinement yielded lattice parameter for the orthorhombic unit cell of $a = 0.7367 \pm 2$ nm, $b = 0.7441 \pm 2$ nm, $c = 0.7702 \pm 2$ nm.

reaction of Al_2O_3 produces $Al_2(WO_4)_3$. In all cases the oxygen deficit is accommodated by nonstoichiometric binary tungsten oxides.

This result is at complete variance with that reported earlier by Pouchard *et al.* who claimed that they had prepared a series of Al_xWO_3 perovskite bronzes (*2, 3*). Unfortunately, their publications do not give preparation details such as heating time, and so we were quite unable to copy their techniques exactly. However, we note that the X-ray powder data for their pseudocubic Al_xWO_3 bronze of approximate composition $Al_{0.1}WO_3$ is very similar to that of the binary tungsten oxide $W_{24}O_{68}$ (*14*) and it is possible that the "bronze" prepared by Pouchard *et al.* is, in fact this selfsame compound. The matter must rest open until more experiments have been tried, but at the moment we conclude that a perovskite bronze Al_xWO_3 does not exist.

In the case of Ga_xWO_3 our evidence is conflicting. A good deal of effort was put into attempting to make a bronze phase, and in a few experiments this apparently succeeded. The results, however, were not wholly reproducible and it did not prove possible to make a series of bronzes with the steadily varying properties that would indicate that such a bronze phase existed. We conclude at the present that stable perovskite bronzes do not exist in the Ga–W–O system under the experimental conditions that we employed. However, it may be that intermediate phases which are similar to such bronzes do occur during the reaction, although our only evidence for this is the presence of orthorhombic and tetragonal phases revealed by powder X-ray diffraction, and we have no evidence that these phases contain Ga or have bronze-like properties.

In the In–W–O system the situation is clear. A perovskite bronze phase forms for low In contents. At temperatures of the order of 1073 K this is tetragonal while at 1373 K it is orthorhombic. The transition between the two forms seems to be reversible and to occur at about 1073 K. The composition range of this phase is very narrow, and a significant phase range for this compound was not found. The most easily formed phase at the temperatures of our preparations possessed the HTB structure. The phase range of this material was from $In_{0.2}WO_3$ to $In_{0.33}WO_3$. Electron microscopy revealed a variable tunnel filling, but we did not explore ordering of the In in the *c* direction, that is, along the tunnels themselves.

A significant result is that no intergrowth tungsten bronzes appear to form under the conditions of our experiments. In fact the In_xWO_3 system is the only tungsten bronze system known to date which supports an HTB phase but which does not make use of an intergrowth region between the lower end of the HTB range and WO_3 to further accommodate composition variation.

Tungsten Bronze Formation

In the past we have used a plot of ionic size versus electronegativity in order to sort the ternary *M*–W–O systems into those which form tungsten bronzes and those that do not (*1*). Although the ionic size used in this plot, the octahedral radius of Shannon and Prewitt (*17*) is in no way a realistic size for the *M* atoms in an M_xWO_3 bronze, the plot worked well. This is because the ionic radius is a useful scaling parameter and was taken as such. From this data it is then found that Al and Ga lie in the region where *CS* phases form and no stable bronzes are to be expected, while In lies in the bronze-forming region.

A problem with this type of sorting diagram is that it is sometimes difficult to assign an "ionic" state to the interpolated *M* atom especially when there are lone pair ions. For example, it is difficult to be certain whether In should be In^{1+} or In^{3+} and, for In^{1+}, it is difficult to assign a realistic

octahedral radius. This then introduces uncertainty into the correct size to be used in estimating the bronze forming tendencies of the atom under discussion. Moreover, electronegativity is not a well-defined quantity, and does not readily separate ions. For example, Al and In are different chemically and yet are listed as having the same electronegativity (*18*).

In order to improve the sorting of the bronzes and arrive at a better understanding of tungsten bronze formation we have investigated other possible parameters, which we list here. Perhaps, as the bronzes are metallic, the most natural first step to take is to replace the octahedral ionic with a metallic radius. There are a number of such metallic radii to use, and we have derived our own from molar volume data, and also used the metallic radii derived in a similar way by Teatum *et al.* (*19*). Similarly, in order to amend the electronegativity factor, we have considered the free energy of formation of oxides. This is because an alternative to the bronze-forming reaction

$$x\,M + WO_3 \rightarrow M_xWO_3$$

is

$$x\,M + WO_3 \rightarrow xMO_n + WO_{3-n\,x}$$

and for stable oxides such as Al_2O_3, this is likely to dominate the chemistry. In the same way we can note that small ions in such oxides have a preference for an octahedral coordination, which would make substitution into WO_3 a realistic alternative to bronze formation, as appears to happen in the case of the Ti_xWO_3 system (*20*).

None of these alternative parameters is able to sort the bronze-forming tendencies any better than that already used. However, all are implicit in the Periodic Table and it seems reasonable, therefore, to display the bronze structures in terms of the Table, and this has been done in Fig. 3. Although the size effect tends to be obscured here, Ba being near to Na in size, for example, it is seen that the type of bronzes formed by the elements is quite well displayed.

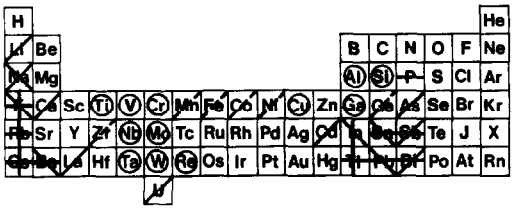

FIG. 3. Periodic Table of the elements showing the extent of tungsten bronze formation, M_xWO_3, for metals M. The symbols represent: (/) stable perovskite bronze; (⁄́) unstable perovskite bronze; (\) tetragonal tungsten bronze; (|) hexagonal tungsten bronze; (—) intergrowth bronzes; (○) no stable bronze formed. Elements not marked have not been investigated in detail.

This organization of data does show some interesting features and suggests trends that have not been noted before. If we consider the left-hand side of the Periodic Table, we note that Ba shows an intergrowth bronze phase. A comparison with the alkali metals, bearing in mind that sizes are not well portrayed, suggests that a bronze Sr_xWO_3 may form and that it is most likely to be a perovskite bronze. Ca and Mg however, would seem less likely candidates. Toward the right-hand side we note that Sb, Pb, and Sn all form intergrowth bronzes. Surprisingly, in the past, Bi has been found not to form an intergrowth bronze but a perovskite phase (*21*). This observation has been modified by recent electron microscope studies of Bi_xWO_3 bronzes where an intergrowth structure was observed (*22*). The major differences between the two results is due to temperatures of preparation and indicate that the perovskite phase may be preferred to an intergrowth phase at higher temperatures. It is known that the Ba, Sn, and Pb intergrowth bronzes are all unstable, but the high-temperature phase region has not been described in detail. It may well be, therefore, that in these systems a high-tempera-

ture perovskite bronze region forms over a narrow stoichiometry range close to the intergrowth composition region. In the same way, it now seems possible that an intergrowth bronze may form in the In_xWO_3 system at lower temperatures. In addition it seems that In lies on another borderline, between the perovskite bronzes and the more complex TTB and HTB bronzes formed by the large ions. The fact that it forms a perovskite bronze shows it to have a relatively small size, but the appearance of an HTB phase at increasing In concentration means that its size is able to support this larger framework. It is therefore tempting to suggest that the difference between the perovskite bronze region and the HTB region may be due to a change in valence state, or, more generally to a change in the delocalization of the In outer electron orbitals. Such a change may well be associated with a change in the electronic properties of the bronze from semiconducting to metallic, and as such would be of some interest. Further work to check these and the other possibilities raised in this paper is now underway, and will be reported in the future.

Acknowledgments

KAW is indebted to ICI for financial support and for use of the Philips 400T electron microscope facilities.

References

1. T. Ekström and R. J. D. Tilley, *Chem. Scr.* **16,** 1 (1980).
2. M. Pouchard, F. Berdoulay, and Vandeven, *C.R. Acad. Sci. Paris* **266,** 1066 (1968).
3. D. Vandeven, J. Galy, H. Pouchard, and P. Hagenmuller, *Mater. Res. Bull.* **2,** 809 (1967).
4. R. J. Bouchard and J. L. Gillson, *Inorg. Chem.* **7,** 969 (1968).
5. A. B. Swanson and J. S. Anderson, *Mater. Res. Bull.* **3,** 149 (1968).
6. P. Labbé, M. Goreaud, B. Raveau, and J. C. Monier, *Acta Crystallogr. Sect. B* **34,** 1433 (1978).
7. P. Labbé, M. Goreaud, B. Raveau, and J. C. Monier, *Acta Crystallogr. Sect. B* **35,** 1557 (1979).
8. P. E. Bierstedt, T. A. Bither, and F. J. Darnell, *Solid State Commun.* **4,** 25 (1966).
9. A. Hussain and L. Kihlborg, *Acta Crystallogr. Sect. A* **32,** 551 (1976).
10. B. G. Brandt and A. G. Nord, *Chem. Commun. Univ. Stockholm* No. 5 (1970).
11. J. L. Waring, *J. Amer. Ceram. Soc.* **48,** 493 (1965).
12. D. C. Craig and N. C. Stephenson, *Acta Crystallogr. Sect. B* **24,** 1250 (1968).
13. T. Ekström and R. J. D. Tilley, *J. Solid State Chem.* **19,** 125 (1968).
14. J. Booth, T. Ekström, E. Iguchi, and R. J. D. Tilley, *J. Solid State Chem.* **41,** 293 (1982).
15. T. Ekström and R. J. D. Tilley, *J. Solid State Chem.* **19,** 227 (1976).
16. P. Labbé, personal communication.
17. R. D. Shannon and C. T. Prewitt, *Acta Crystallogr. Sect. B* **25,** 925 (1969); **26,** 1046 (1970).
18. W. Gordy and W. J. O. Thomas, *J. Chem. Phys.* **24,** 439 (1956).
19. E. Teatum, K. Geschneider, and J. Waber, LA-2345, U.S. Dept. of Commerce, Washington, D.C. (1960).
20. T. Ekström and R. J. D. Tilley, *Mater. Res. Bull.* **9,** 705 (1974).
21. M. Parmentier and C. Gleitzer, *C.R. Acad. Sci. Paris, C* **281,** 819 (1975).
22. D. A. Jefferson, M. K. Uppal, J. Gopalakrishnam, A. Ramanan, and C. N. R. Rao, *in* "Solid Chemistry, 1982," (R. Metselaar, H. J. M. Heijligers, and J. Schoonman, Eds.), Elsevier, Amsterdam (1983).